SLAC–PUB–7243
August 1996

High Gradient Experiments on NLCTA Accelerator Structures *

J.W. Wang, J.P. Eichner, K.H. Fant, H.A. Hoag,
R.F. Koontz, T. Lavine, G.A. Loew, R.J. Loewen,
A. Menegat, R.H. Miller, C.D. Nantista, C. Pearson,
R.D. Ruth, S.G. Tantawi, A.E. Vlieks, P.B. Wilson, and C. Yoneda
Stanford Linear Acceleratory Center, Stanford University, Stanford, California

Abstract

This paper presents new results of high-gradient studies performed on a 1.8 m traveling-wave accelerator section with detuned high-order deflecting modes. This structure was designed initially for studies of detuned structures and will be installed in the Next Linear Collider Test Accelerator (NLCTA). The paper describes the test set-up in the Accelerator Structure Test Area (ASTA) including electron gun, pre-buncher, pre-accelerator, spectrometer, Faraday cups, 200 MW SLED-II power compression system, Magic-T type phase shifters and attenuators. Rf processing, detailed dark current analysis, radiation problems, and beam acceleration measurements are discussed.

Presented at the
XVIII International Linac Conference (LINAC96)
CERN, Geneva, Switzerland
26–30 August 1996

*Work supported by the Department of Energy, contract DE–AC03–76SF00515.

High Gradient Experiments on NLCTA Accelerator Structures

J.W. Wang, J.P. Eichner, K.H. Fant, H.A. Hoag,
R.F. Koontz, T. Lavine, G.A. Loew, R.J. Loewen,
A. Menegat, R.H. Miller, C.D. Nantista, C. Pearson,
R.D. Ruth, S.G. Tantawi, A.E. Vlieks, P.B. Wilson, and C. Yoneda
SLAC, Stanford University, USA

Abstract

This paper presents new results of high-gradient studies performed on a 1.8 m traveling-wave accelerator section with detuned high-order deflecting modes. This structure was designed initially for studies of detuned structures and will be installed in the Next Linear Collider Test Accelerator (NLCTA). The paper describes the test set-up in the Accelerator Structure Test Area (ASTA) including electron gun, pre-buncher, pre-accelerator, spectrometer, Faraday cups, 200 MW SLED-II power compression system, Magic-T type phase shifters and attenuators. Rf processing, detailed dark current analysis, radiation problems, and beam acceleration measurements are discussed.

Experimental Setup and Accelerator Section

The Accelerator Structure Test Area (ASTA), where all tests were performed, has been described in a previous paper [1]. Figure 1 shows the layout of the setup for the high power test of the 1.8m traveling-wave section. The accelerating mode of this detuned structure has a uniform phase velocity equal to the speed of light [2]. The electrons from an 80kV thermionic gun are bunched and pre-accelerated in order to be captured in the accelerator section. Both prebuncher and pre-accelerator use single cavities with nose-cones, in order to reduce the transient beam loading effect. The cavities are made of stainless steel to lower their Q value. The rf power for the prebuncher and pre-accelerator is obtained via directional couplers from the feed waveguide for the accelerator section. Each feed includes a Magic-T type attenuator/phase shifter to adjust rf amplitude and phase. Two main arms are assigned to be input and output ports, and two side-arms are shorted with non-contacting plungers driven by stepping motors. Moving the shorts respectively toward the T-junction and away from it changes the phase at a constant amplitude, whereas moving the shorts synchronously in the same direction changes the amplitude at a constant phase.

Several scintillator detectors are installed alongside the accelerator structure for X-ray measurements. The detector heads are made from NaI crystals (0.38 in. in diameter $\times$ 1.0 in. in length) with lead collimation. The photons created by the X-rays are transmitted through a 3-5 ft. optical fiber to a Hamamatsu HC125 PMT based-detector, which includes a divider, high voltage power supply and signal processing circuitry. The whole system is calibrated by using a standard radioactive source.

The 1.8m detuned structure is the first model for the NLC Test Accelerator at SLAC. It has 204 cavities plus input and output couplers. Its characteristics and main rf parameters are shown in the table.

Section length	1.8 m
Phase advance per cell	$2\pi/3$
Iris aperture diameter	1.134–0.786 cm
Cavity diameter	2.228–2.059 cm
Disk thickness	0.1–0.2 cm
Group velocity	$0.12c$–$0.03c$
Filling time	100 ns
Time constant	205–177 ns
Attenuation parameter	0.498 nepers
Shunt impedance	66.48–83.40 MΩ/m
Factor of merit, Q	7416–6674
Peak power for 50 MV/m	86.5 MW
RF pulse length	150 ns
Peak input power	150 MW
Maximum E_{acc}	80 MV/m
Average E_{acc}	67 MV/m
Maximum surface E_s	159 MV/m
E_s/E_{acc}	2.37

Experimental Results

RF processing was performed in two stages. The first stage took place in March of 1994, over a period of 30 hours in a two-day period, to reach an average accelerating gradient of 50 MV/m. The second stage took place in June of 1995 after the installation of a 50 MW peak power klystron. The improved SLED-II system was able to produce 200 MW, 150 ns rf pulses. The maximum power delivered to the accelerator structure was 150 MW, and the maximum accelerating gradient was limited by the klystron output power. Figure 2 shows the straight-ahead dark current as a function of accelerating gradient. Significantly higher power is needed to further reduce this dark current [3]. The dark current spectrum obtained so far was measured using the 45° spectrometer. In order to obtain more information on the origin of the captured dark current, two dipole magnets were installed along-

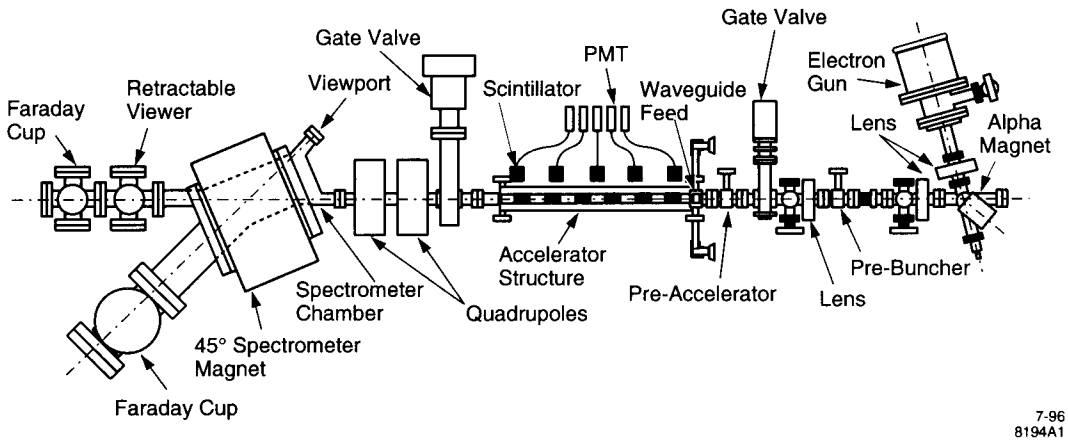

Figure 1: Layout of Accelerator Structure Test Area.

side the accelerator section at a given z-position. They can create about 600 Gauss of transverse magnetic field in "x" and "y" to prevent any dark current originating upstream from reaching the spectrometer. Hence, each curve in Fig. 3 is a spectrum of the dark current transmitted and collected from that part of the accelerator section downstream of the magnets. Figure 4 shows the total dark current collected at the straight-ahead Faraday cup as a function of the magnets position. From these plots we can conclude that most of the dark current is composed of low energy electrons. The total number of electrons captured at the end of the accelerator section no longer increases when the magnets are located upstream of cavity No. 90. This is probably because when the field emitted electrons are accelerated or decelerated by the rf fields, a majority of them strike the cavity walls. Secondary or back-scattered electrons are then created, which are also accompanied by X-ray radiation. During rf processing, the outputs of the scintillator-PMT system give strong bursts if there is sparking at nearby cells. Figure 5 gives the waveforms of four X-ray detectors at two different rf power levels. In the test, scintillators 1, 2, 3, and 4 are located respectively at the input region, one third, two third, and the output region of the accelerator section. Figure 6 shows the radiation dosage as a function of the position along the accelerator section at two different gradients.

A beam test was performed at an average accelerating gradient of 50 MV/m. The rf pulse length was 150 ns for the SLED-II system and the filling time of the structure was 100 ns. Because of radiation safety limitations, a pulsed beam of only 40 mA, 30 nsec was used. The maximum rf power available to the pre-accelerator was

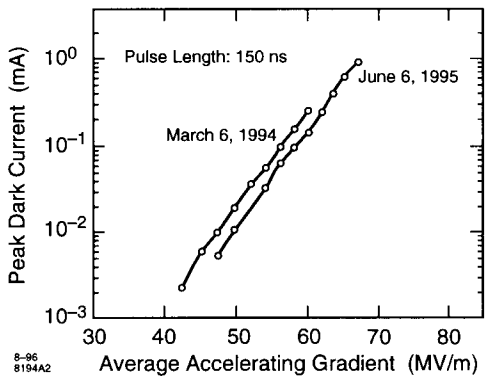

Figure 2: Peak dark current measured by a straight-ahead Faraday cup as a function of average accelerating gradient for two stages of rf processing.

lower than expected because of the rf loss in the waveguide system. The operating frequency was adjusted slightly higher to allow the captured electrons to drift in phase toward the rf peak in order to increase the net acceleration. The electron energy gain showed that for the particles on the rf peak, the average accelerating gradient for an input power of 90 MW reached 50 MV/m.

Work supported by the Department of Energy, contract DE–AC3–76SF00515.

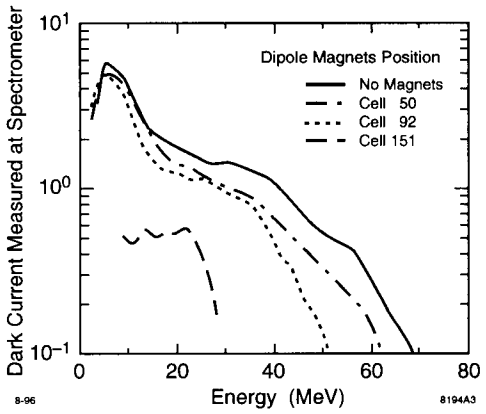

Figure 3: Energy spectrum of dark current at average accelerating gradient of 58 MV/m for different positions of the dipole magnets.

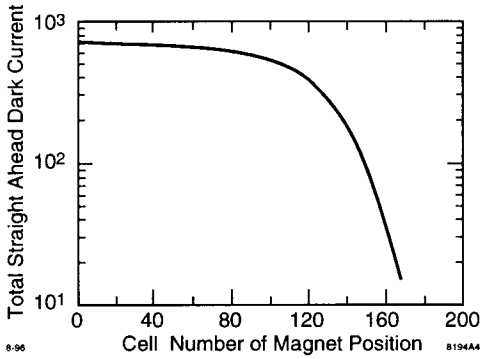

Figure 4: Total dark current collected at the straight-ahead Faraday cup as a function of the position of the dipole magnets.

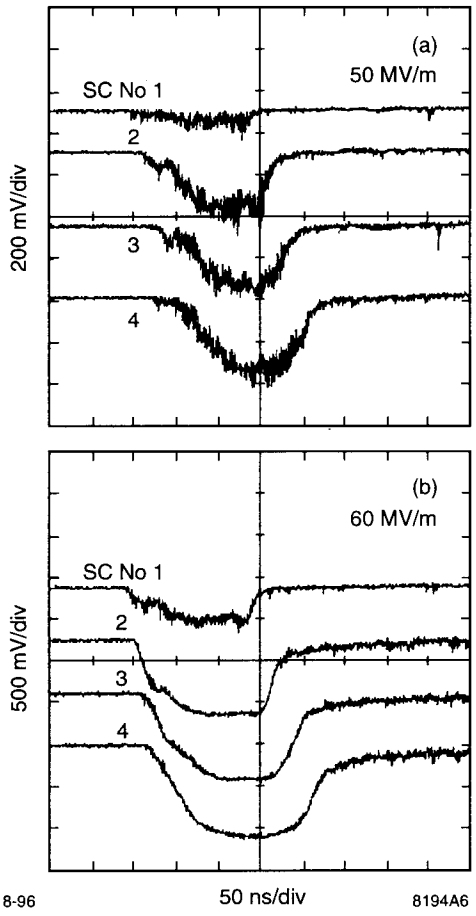

Figure 5: Waveforms for four X-Ray detectors at two different average accelerating gradients: (a) 50 MV/m, (b) 60 MV/m.

References

[1] J. W. Wang et al, "High Gradient Tests of SLAC Linear Accelerator Structures," LINAC94, Tsukuba, Japan, August 1994; SLAC-PUB-6617 (1994).

[2] J. W. Wang and E. M. Nelson, "Design of the Detuned Accelerator Structure", PAC93, Washington, DC, May 1993; SLAC-PUB-6142 (1993).

[3] G. A. Loew and J. W. Wang, "RF Breakdown Studies in Room Temperature Electron Linac Structures," 13th Int. Symp. on Discharges and Electrical Insulation in Vacuum, Paris, France, 1988, SLAC-PUB-4647 (1988).

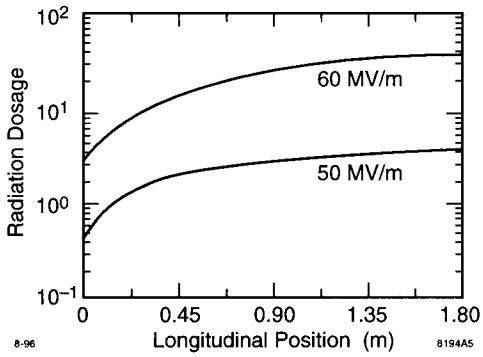

Figure 6: Radiation dosage along the accelerator section at two different average gradients.